AD-A097 991   NAVAL RESEARCH LAB   WASHINGTON DC   F/G 20/8
SIMULATION OF LASER BEAM NONUNIFORMITY EFFECTS.(U)
APR 81   M H EMERY, J H ORENS, J H GARDNER
UNCLASSIFIED   NRL-MR-4500   NL

END
DATE
FILMED
9-81
DTIC

(14) NRL-MR-4500

REPORT DOCUMENTATION PAGE	READ INSTRUCTIONS BEFORE COMPLETING FORM
1. REPORT NUMBER NRL Memorandum Report 4500	2. GOVT ACCESSION NO. AD-A097991	3. RECIPIENT'S CATALOG NUMBER

4. TITLE (and Subtitle) SIMULATION OF LASER BEAM NONUNIFORMITY EFFECTS	5. TYPE OF REPORT & PERIOD COVERED Interim report on a continuing NRL problem.
	6. PERFORMING ORG. REPORT NUMBER

7. AUTHOR(s) M. H. Emery J. H. Orens* J. H. Gardner and J. P. Boris	8. CONTRACT OR GRANT NUMBER(s)

9. PERFORMING ORGANIZATION NAME AND ADDRESS Naval Research Laboratory Washington, DC 20375	10. PROGRAM ELEMENT, PROJECT, TASK AREA & WORK UNIT NUMBERS 44-0575-0-1; NPO 10501

11. CONTROLLING OFFICE NAME AND ADDRESS Department of Energy Washington, DC	12. REPORT DATE April 1981
	13. NUMBER OF PAGES 22

14. MONITORING AGENCY NAME & ADDRESS(if different from Controlling Office)	15. SECURITY CLASS. (of this report) UNCLASSIFIED
	15a. DECLASSIFICATION/DOWNGRADING SCHEDULE

16. DISTRIBUTION STATEMENT (of this Report)

Approved for public release; distribution unlimited.

17. DISTRIBUTION STATEMENT (of the abstract entered in Block 20, if different from Report)

18. SUPPLEMENTARY NOTES

*Present address: Berkley Research Associates, Springifield, VA 22151

19. KEY WORDS (Continue on reverse side if necessary and identify by block number)

Laser driven ablation layers
Accelerating foils
Computational fluid dynamics
Laser fusion

Laser nonuniformities

20. ABSTRACT (Continue on reverse side if necessary and identify by block number)

We investigate the effect of a nonuniform beam on the ablative acceleration of thin foils using the FAST2D laser-shell simulation code. The results show that laser nonuniformities with scalelengths greater than the distance from the ablation surface to the critical surface would have a severe impact on drive pressure symmetry and hence on pellet gain.

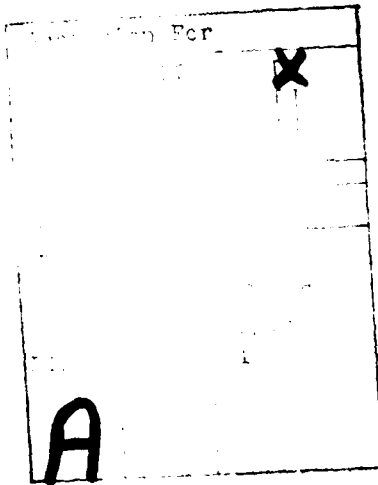DD FORM 1473 EDITION OF 1 NOV 65 IS OBSOLETE
1 JAN 73
S/N 0102-014-6601

251950

CONTENTS

SIMULATION OF LASER BEAM NONUNIFORMITY EFFECTS

I. Introduction:

In laser fusion, spherical layered pellets are imploded through laser induced ablation of the outer surface. The laser energy is absorbed near the critical density and the heat is conducted inward to the cold ablator material. The heated material expands outward and the remaining cold material is accelerated inward as a result of momentum conservation. In order to achieve the densities and temperatures required for thermonuclear fusion, this inward acceleration must be very symmetric over the surface of the pellet. For laser fusion to be practical, the laser energy must be efficiently coupled to the pellet. Implosion symmetry and energy efficiency may be conflicting requirements.

Experiments and theory at NRL[1] and elsewhere[2] indicate that the most efficient laser energy coupling occurs at relatively low irradiances $(10^{13} - 10^{14}$ Watts/$_{cm}2)$. These low irradiances require thin-shelled pellets[3] (of thickness ΔR) to be accelerated over large distances (R) such that $R/\Delta R \gtrsim 10$. This places severe requirements on ablation pressure uniformity $(\Delta p/p \lesssim 1\%)$ if high gain is to be achieved.[4] One of the major causes of ablation pressure nonuniformity is nonuniformity of the laser beam intensity. The problem we address in this report is the relation between nonuniformities in the laser beam intensity and nonuniformities in the ablation pressure of thin planar targets as a function of laser intensity and scalelength of the inhomogeneity. These thin planar targets model one section of a large radius thin shell pellet.

An illustration of the laser-target interaction is given in Figure 1. The distance from the ablation surface, the region of steepest density

gradient and where the pressure is "applied", to the critical surface, where the energy is absored, is D_{ac}. The scale length of the inhomogeneity in laser intensity is λ_{ℓ}. If the distance from the ablation surface to the critical surface is much larger than the scalelength of this inhomogeneity (i.e., $D_{ac} \gg \lambda_{\ell}$) then lateral energy flow should smooth out the inhomogeneity before it reaches the ablation surface.[5] If $D_{ac} \ll \lambda_{\ell}$, then the inhomogeneity should imprint itself on the target and the variation in ablation pressure should be of the same order as the variation in laser intensity. This inhomogeneity in ablation pressure will, in turn, affect the target velocity and acceleration profiles.

Theory[6] and experiment[7] indicate that the distance from the ablation surface to the critical surface is directly proportional to the intensity of the laser. Here we determine the extent to which lateral energy flow can smooth out laser inhomogeneities as a function of laser intensity.

In the next section we discuss our model. Section III contains the results of the simulation with the summary and conclusions in Section IV.

II. The Model:

We model the effect of an inhomogeneous laser beam on a thin (15μm thick) plastic (CH) foil with the FAST2D[8,9] laser-shell simulation code. This is a fully two-dimensional Cartesian code with a sliding Eulerian grid. It solves the ideal hydrodynamic equations using the flux-corrected transport (FCT)[10] algorithms with a two-dimensional classical plasma thermal conduction routine. The thermal conduction coefficient has the classical $K_0 T^{5/2}$ temperature dependence where K_0 is the standard Braginskii coefficient,[11] 3.06×10^8 erg/(cm-sec-ev$^{7/2}$).

The grid is initially uniform in the region of the foil. Inside (opposite the laser) and outside (the underdense plasma) of this region the grid is stretched. The inside region is filled with a very low density plasma having the same adiabat as the target plasma. On the outside, beyond the critical surface, both the density and pressure drop off exponentially. The system is periodic in the transverse direction.

All the laser energy is assumed to be absorbed through resonant absorption. The laser flux is introduced as an energy source in the heat equation and is deposited into the two cells about the critical density. The plasma is assumed to be fully ionized.

The initial density, pressure and temperature profiles are generated from a one-dimensional, analytic, quasi-static equilibrium solution of a set of hydrodynamic equations that model a laser-plasma interaction.[12] The solutions have been shown to have provided an adequate steady state with a one-dimensional laser-foil computer code.[13] A representative initial profile is illustrated in Figure 2. The initial conditions are assumed uniform in the transverse direction of the foil. A two-dimensional perspective plot of the density is given in Figure 3.

Laser beam profiles are typically Gaussian with inhomogeneities manifesting themselves by a reduced intensity in the center of the beam. See Figure 4. Since we are only interested in the effect of laser beam asymmetries, we invoke the periodicity of the code and model only the peak-to-peak variation in intensity. λ_ℓ is the scale length of the inhomogeneity. The results of a parameter variation in laser intensity and scalelength of the inhomogeneity are presented in the next section.

III. Results:

Three different average laser intensities, $\langle I \rangle = 5 \times 10^{12}$, 1×10^{13} and 2×10^{13} W/cm^2 are used with the scalelength of the inhomogeneity ranging between 100 microns and 600 microns. For all the results presented here the variation in intensity is 80% ($\frac{\Delta I}{\langle I \rangle} = 0.80$, $\Delta I = I_{max} - I_{min}$) and the laser wavelength is 1.06 μm. Data are shown at 3 and 6 nanoseconds.

Figure 5 shows the variation in the ablation pressure as a function of the scalelength of the inhomogeneity for the three intensities after 3 nanoseconds. Note that the large scalelength variation ($\lambda_\ell = 600$ μm) severely impacts the target for all three intensities. For Case A, $\langle I \rangle = 5.0 \times 10^{12}$ W/cm^2, lateral energy flow has no significant impact for scalelength greater than 100 μm whereas for Case C, $\langle I \rangle = 2.0 \times 10^{13}$ W/cm^2, lateral flow gives rise to only a 5% pressure variation for $\lambda_\ell = 500$ μm.

In Figures 6-9, we present a detailed look at the foils for Case B, $\langle I \rangle = 1.0 \times 10^{13}$ W/cm^2, with $\lambda_\ell = 100$ μm and 600 μm. A perspective plot of the density at $T = 6 \times 10^{-9}$s for $\lambda_\ell = 600$ μm is shown in Figure 6. As can be seen, the ablation rate variation follows the laser intensity variation and the foil becomes severely distorted and is beginning to buckle. Figure 7 illustrates the pressure contours at the same time. Here the laser light is coming from the right. The lines are contours of constant pressure in 0.10 increments counting from the outside inward. The ablation surface and critical surface are also indicated. Note the pockets of very high pressure at the "edges" of the ablation surface. These are, of course, the regions of highest laser intensity.

The density plot for $\lambda_\ell = 100$ μm is given in Figure 8. Here there is negligeable distortion of the foil. The corresponding pressure contours

are presented in Fig. 9. In this case the ablation surface is essentially

equivalent to a contour surface. Lateral energy flow has provided

enough smoothing to produce only a 0.5% variation in the ablation pressure.

IV. Summary and Conclusion:

The numerical results are summarized in Figure 10, where the variation

in ablation pressure is plotted as a function of the average laser

intensity for all six scalelengths. This is equivalent to plotting the

variation in ablation pressure as a function of the average distance

between the ablation surface and the critical surface as indicated on the

graph. The direct correlation between D_{ac} and the laser intensity has

also been noted experimentally[7] and theoretically.[6]

Lateral energy flow in the form of transverse thermal conduction

does tend to smooth the effects of laser beam nonuniformities. The degree

of smoothing is directly related to the distance from the ablation surface

to the critical surface.[14] To smooth non-uniformities to the extent that

the ablation pressure variation is less than 1% requires that $D_{ac} \sim 0 \, (\lambda_{\ell})$.

This result is somewhat intuitive in that if the scalelengths of temperature

variations are comparable, a thermal wave propagating transverse to the

laser beam should smooth out moderate temperature variations at about the

time that the laser energy has been conducted to the ablation surface.

Detailed one-dimensional numerical results[6] indicate that the scaling

for the distance from the ablation surface to the critical surface has

the following relation

$$D_{ac} \alpha \; (I/\omega^3)$$

where ω is the frequency of the laser light. The results presented here give

the same scaling with intensity and indicate that laser intensity variations can

be smoothed so that they have a negligeable impact on the target as long as the scalelength of the inhomogeneity is comparable to the distance from the ablation surface to the critical surface.

These results indicate that laser asymmetries must be considered in the design of a reactor-size laser fusion system. Employing state-of-art techniques, it is unlikely that the illumination uniformity of the target plane would be much better than 40%.[15] Using a many beam system with severe overlap, each beam would have a spotsize on the order of the target radius[16] (2-3mm), giving rise to intensity variations of the same order. To smooth intensity variations with a 2-3mm scalelength would require laser intensities on the order of $2-3 \times 10^{14}$ W/cm^2, assuming a $1.06 \mu m$ laser. (Since the density falls off much more rapidly in spherical geometry than in slab geometry, the required intensity to give $D_{ac} \approx 3mm$ is likely to be even greater than $3 \times 10^{14} W/cm^2$). The benefits of increased smoothing must then be balanced against poor absorption and plasma instabilities that occur at high irradiances. It would seem that the most likely means to increase the distance from the ablation surface to the critical surface is to reduce the frequency of the laser light,[14,15] contrary to the current lines of research.[17]

The results obtained here are qualitatively similar to the experimental results obtained at NRL where opaque strips were used to perturb the laser intensity.[18]

References

1. NRL Laser-Plasma Interaction Group, NRL Memo Report No. 3890 (1978), ed. B. H. Ripin; R. Decoste et al., Phys. Rev. Lett. 42, 1973 (1979); B. H. Ripin et al., Phys. Rev. Lett. 43, 350 (1979); B. H. Ripin et al., Phys. Fluids 23, 1012 (1980).

2. O.N. Krokhin et. al., Sov. Phys. JETP 42, 107 (1976); N.G. Basov et. al., Sov. Phys. JETP Lett. 26, 433 (1977); J. P. Anthes, M. A. Gusinow, and M. Keith Matzen, Phys. Rev. Lett. 41, 1300 (1978).

3. Y. V. Afanasev et al., Zhetf Pis Red 21, 150 (1975).

4. J. H. Nuckolls et al., European Conference on Laser Interaction with Matter, 1977.

5. J. Nuckolls et al., Nature 239, 139 (1972).

6. J. H. Gardner et al., Bull. Am. Phys. Soc. 25, 949 (1980).

7. J. Grun et al., Bull. Am. Phys. Soc. 25, 932 (1980); J. Grun et al., NRL Memo Report No. 4410 (1980) (Submitted to Phys. Rev. Lett.).

8. J. P. Boris, Comments on Plasma Physics and Controlled Fusion, 3.1 (1977).

9. J. P. Boris, NRL Memorandum Report 3427, 1976.

10. J. P. Boris and D. L. Book, "Methods of Computational Physics" 16, 85 (1976).

11. S. I. Braginskii, "Reviews of Plasma Physics" 1, 205, ed. by A. Leontovich (Consultants Bureau, New York, 1965).

12. J. H. Orens, "Accurate Analytic Approximations and Numerical Solutions for the Structure of Quasi-Static Laser Driven Ablation Layers", NRL Memo report 4167 (1980).

13. P. J. Moffa et al., Bull. Am. Phys. Soc. 24, 946 (1979).

14. Mark H. Emery et al., Bull. Am. Phys. Soc. 25, 947 (1980).

15. S. Bodner, "Critical Elements of High Gain Laser Fusion", NRL Memo Report No. 4453 (1981).

16. B. Ripin, private communication.

17. C.E. Max, Bull Am. Phys. Soc. 25, 992 (1980); E. Fabre, Bull Am. Phys. Soc. 25, 992 (1980); D.C. Slater, Bull Am. Phys. Soc. 25, 992 (1980).

18. B. H. Ripin, et al., Bull. Am. Phys. Soc. 25, 946 (1980); S. P. Obsenchain et al., "Beam Nonuniformity Effects on Laser Ablatively Accelerated Targets", NRL Memo Report No. 4309 (1980).

Acknowledgments
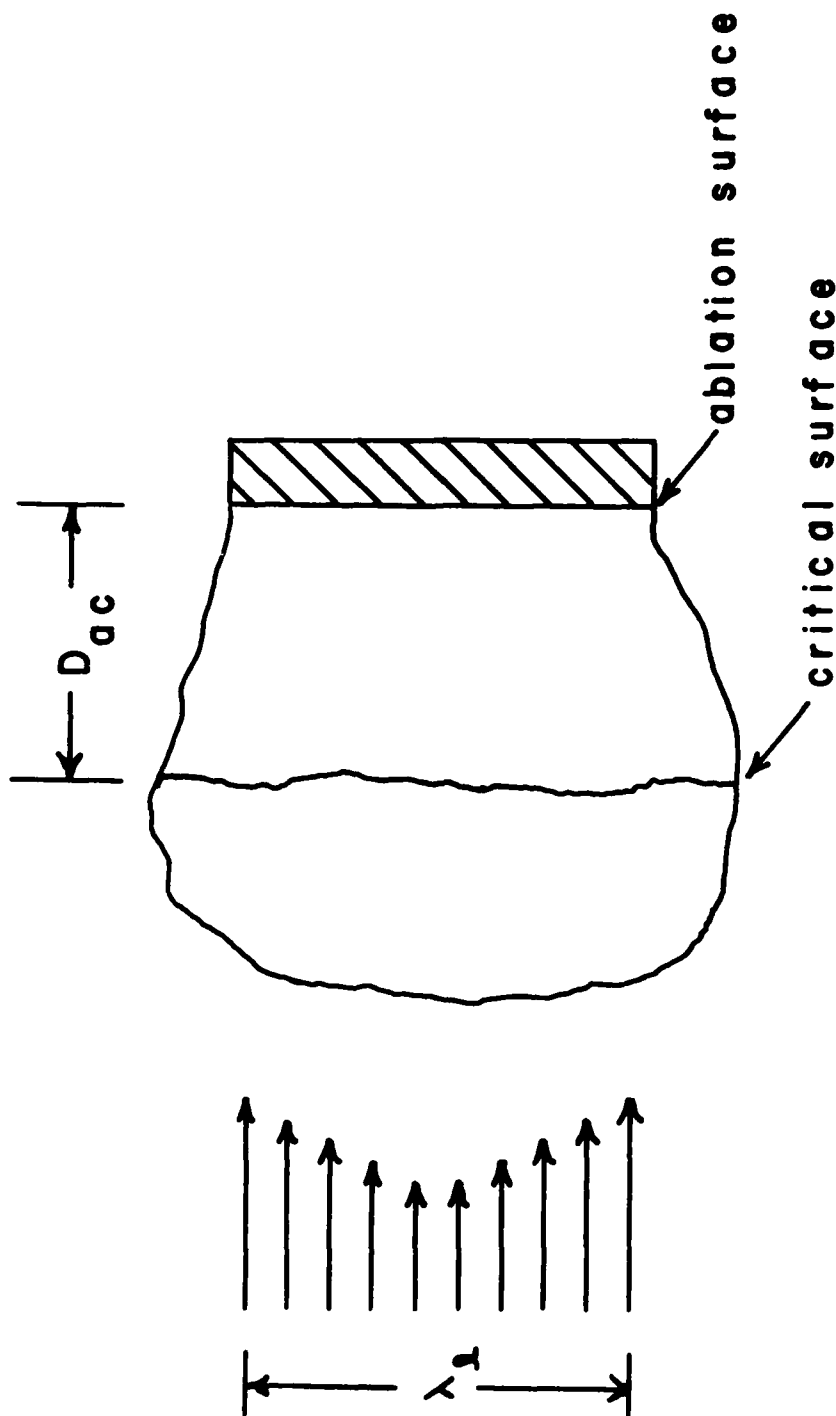
Fig. 1 - A sketch of the laser-foil interaction, D_{ac} is the distance from the ablation surface to the critical surface. λ_ζ is the scalelength of the laser intensity variation.

11
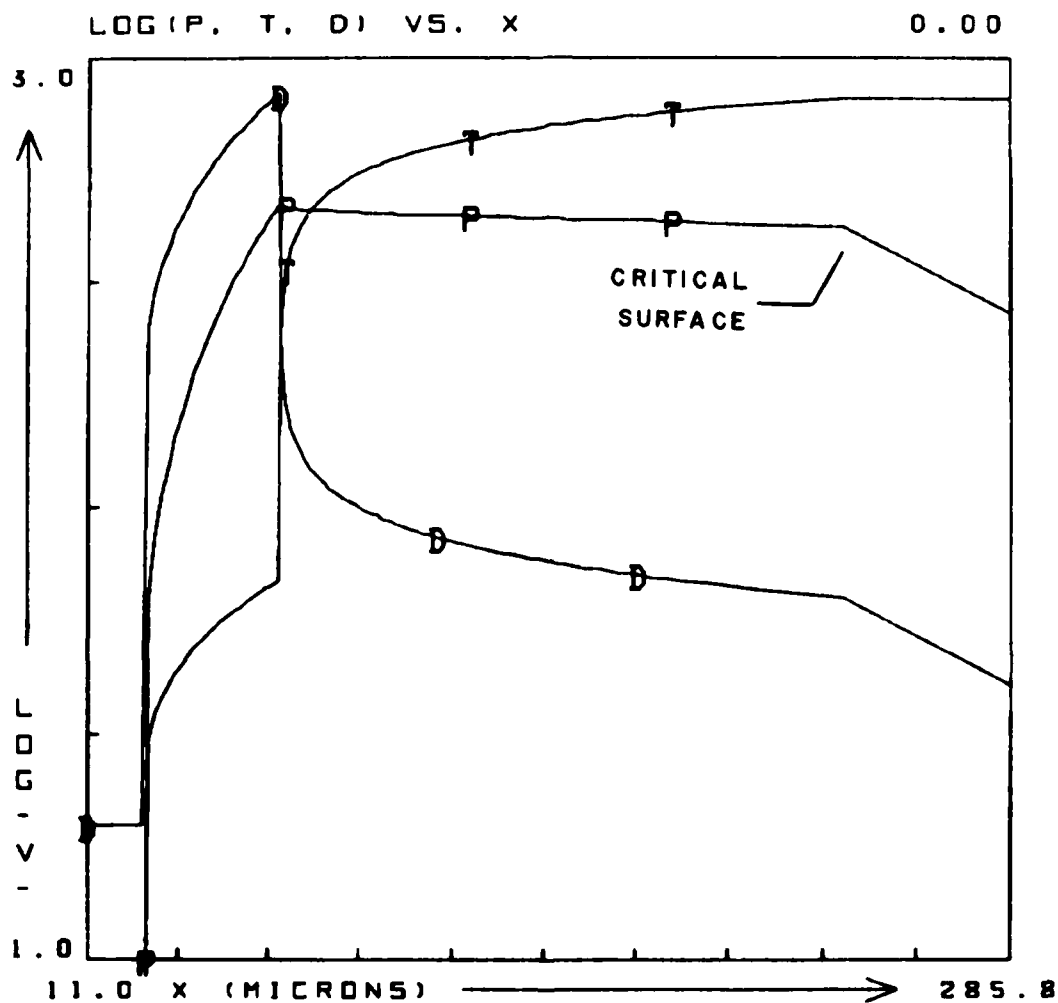
Fig. 2 - A semi-log plot of the initial pressure, density
         and temperature profiles of a thin plastic foil.

FAST2D LASER SHELL 0.00•10 °
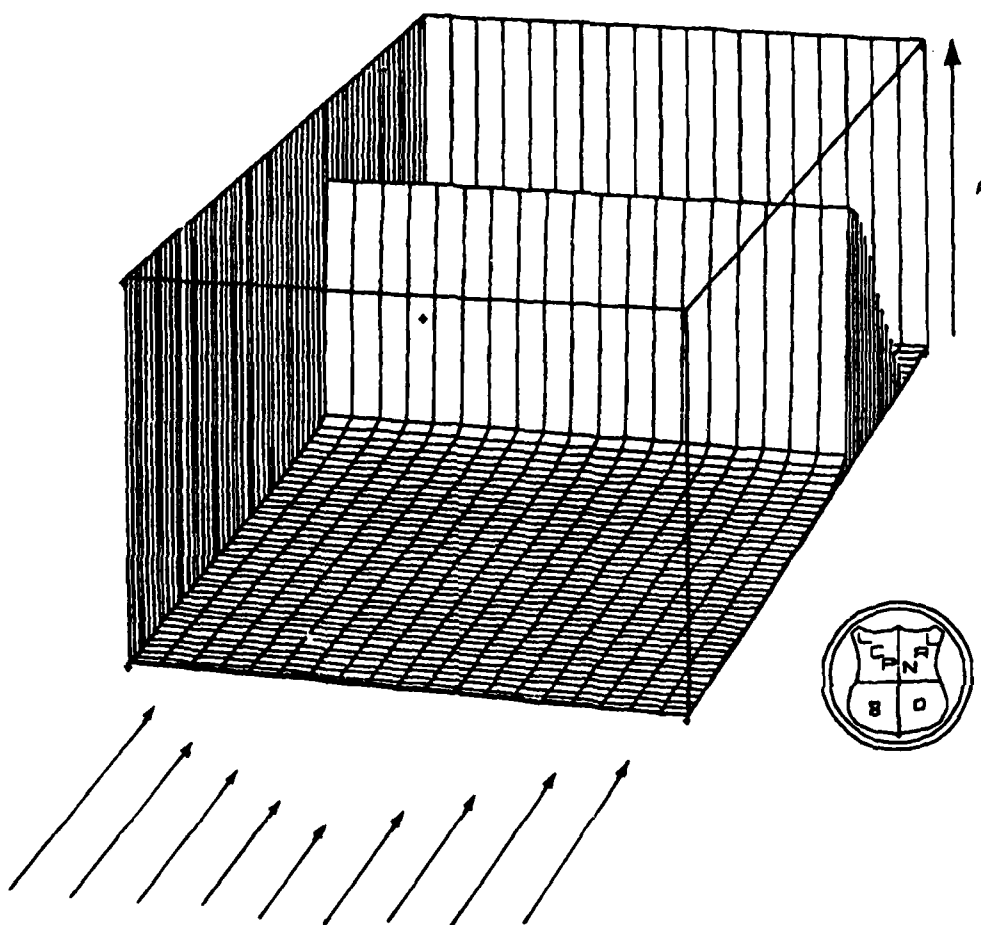
Fig. 3 - A two-dimensional perspective plot of the initial mass density. The laser beam is coming in from the front with an inhomogenity scale-length of λ_ℓ transverse to the direction of propagation.
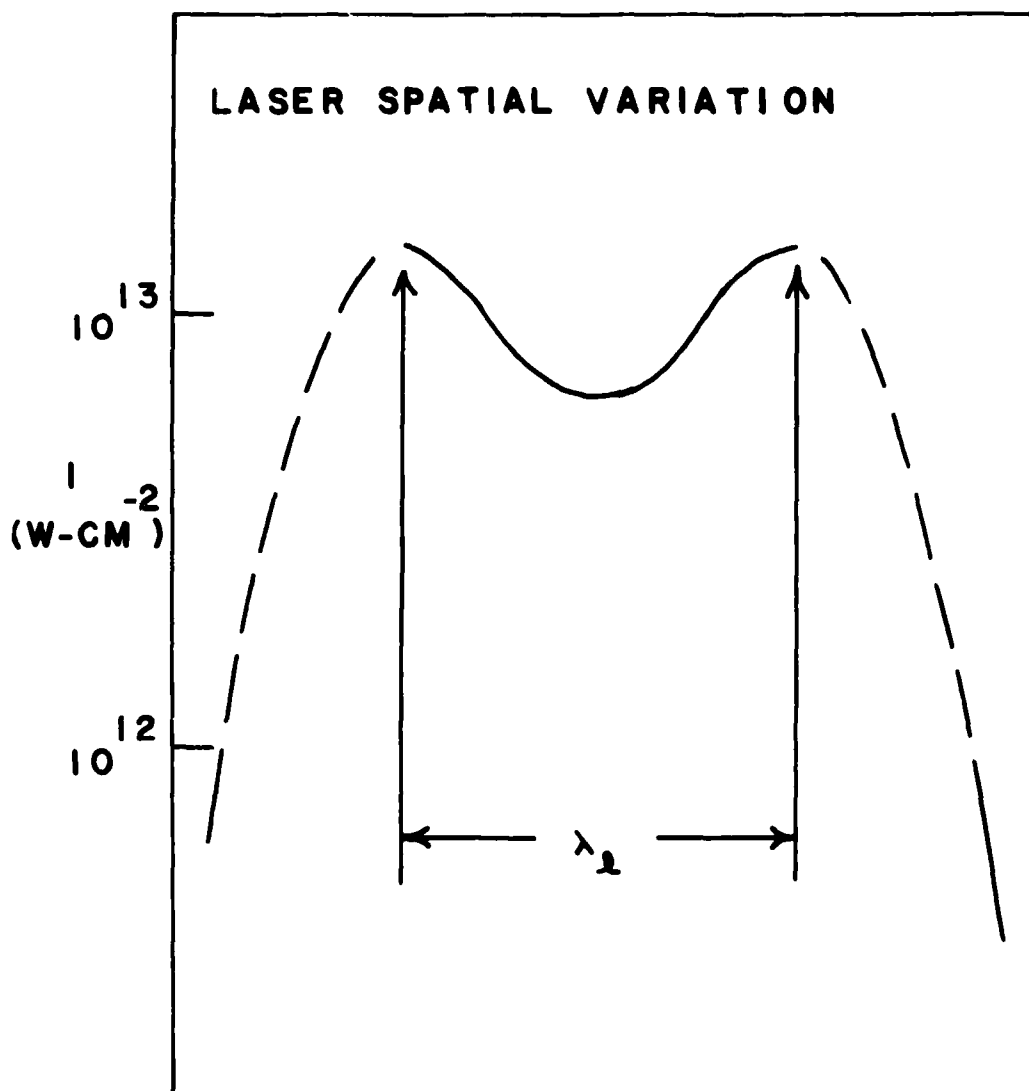
Fig. 4 - A typical example of the spatial variation of the laser intensity. We model only the region spanned by the distance λ_ℓ.

14
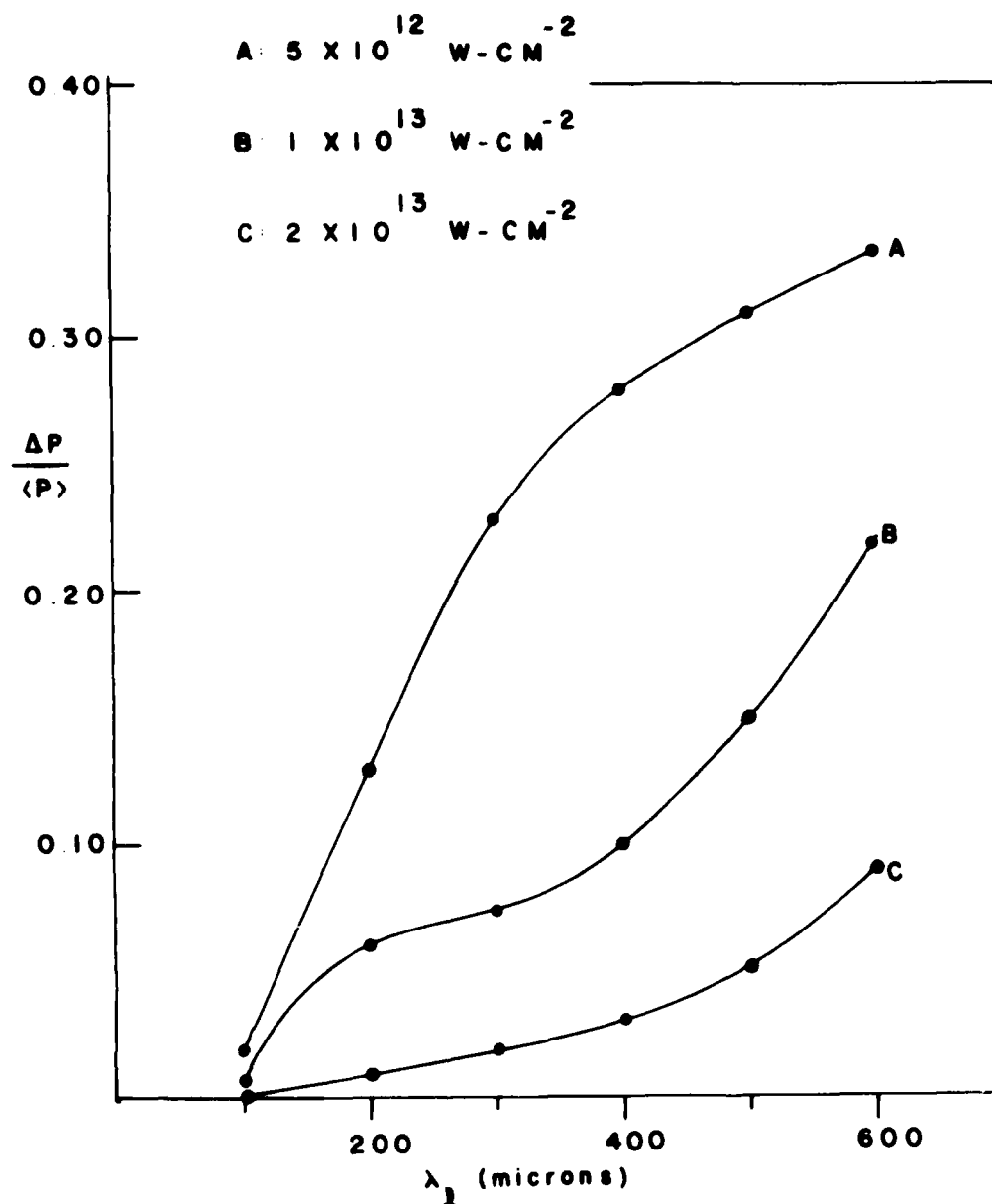
Fig. 5 - The variation in ablation pressure ($\Delta p/\langle p \rangle$) as a function of the scale-length of the inhomogeneity ( ) for three different average laser intensities ($\langle I \rangle$ = 5.0 x 10^{12}, 1.0 x 10^{13} and 2.0 x 10^{13} W/cm^2). $\Delta I/\langle I \rangle$ =0.80 for all three intensities.

FAST2D LASER SHELL   6.00*10^{-9}
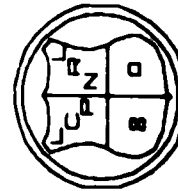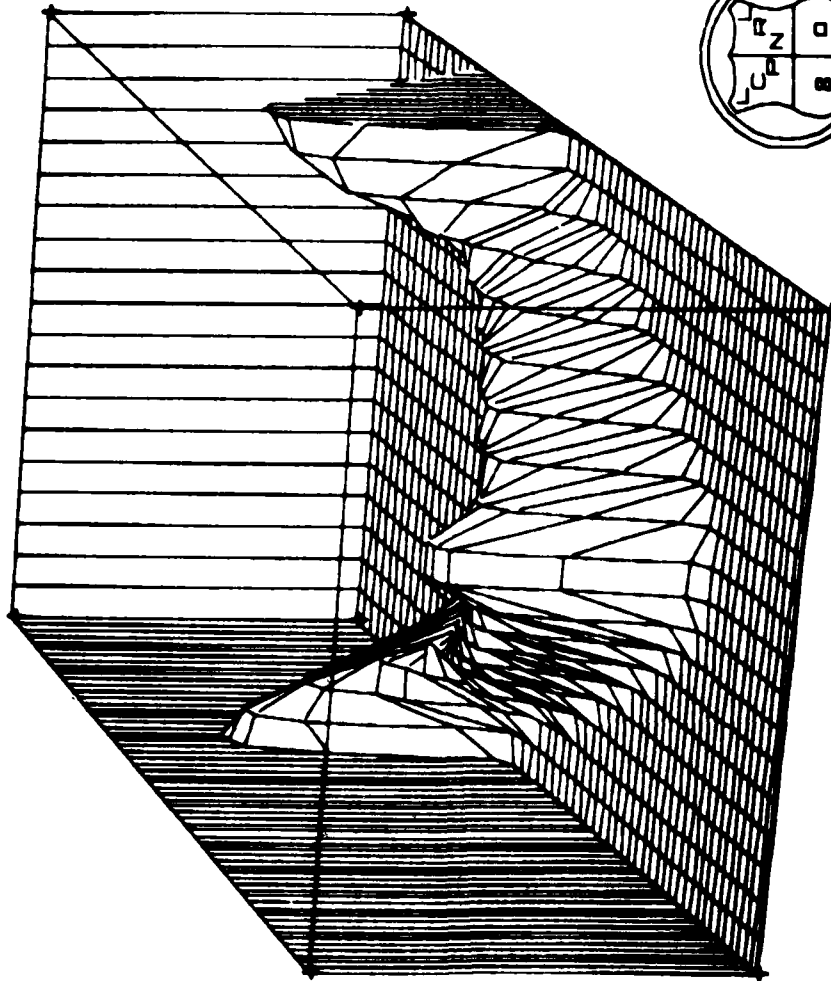
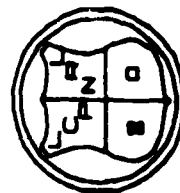$\langle I \rangle = 1.0 \times 10^{13}$ W/cm^2

$\lambda_{\ell} = 600 \mu$m
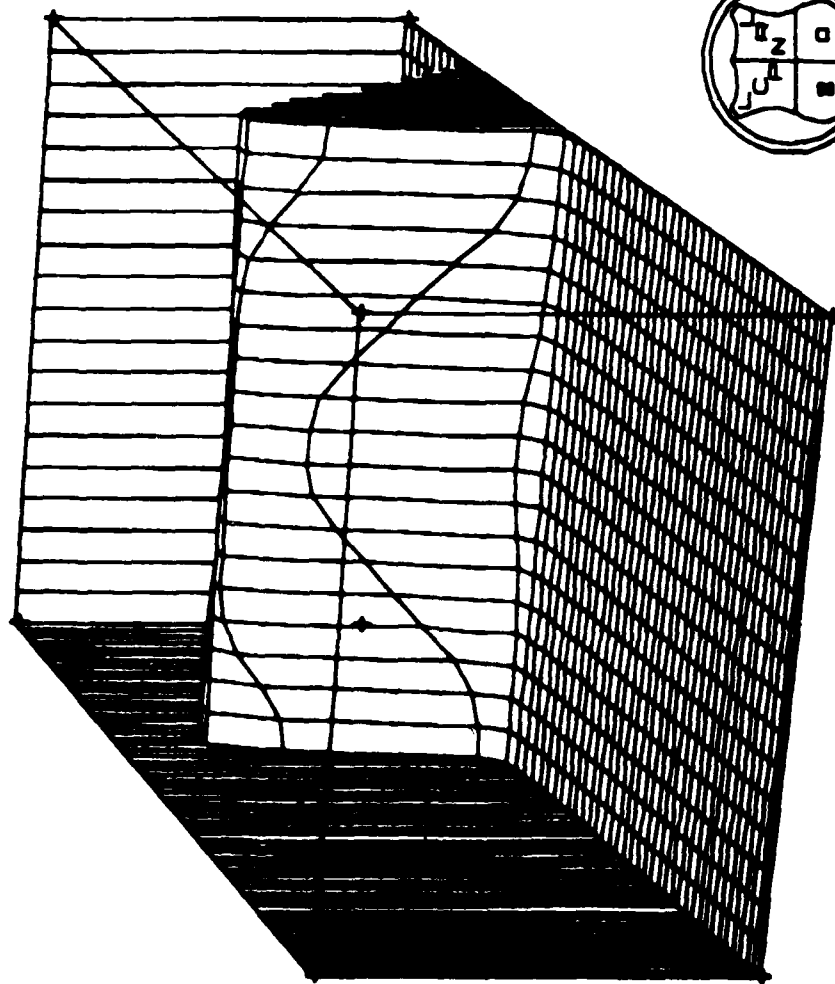
Fig. 6 - The perspective density plot for $\langle I \rangle = 1.0 \times 10^{13}$ W/cm^2 amd $\lambda = 600$ μm after 6 nanoseconds. The foil is severely distorted and beginning to buckle.
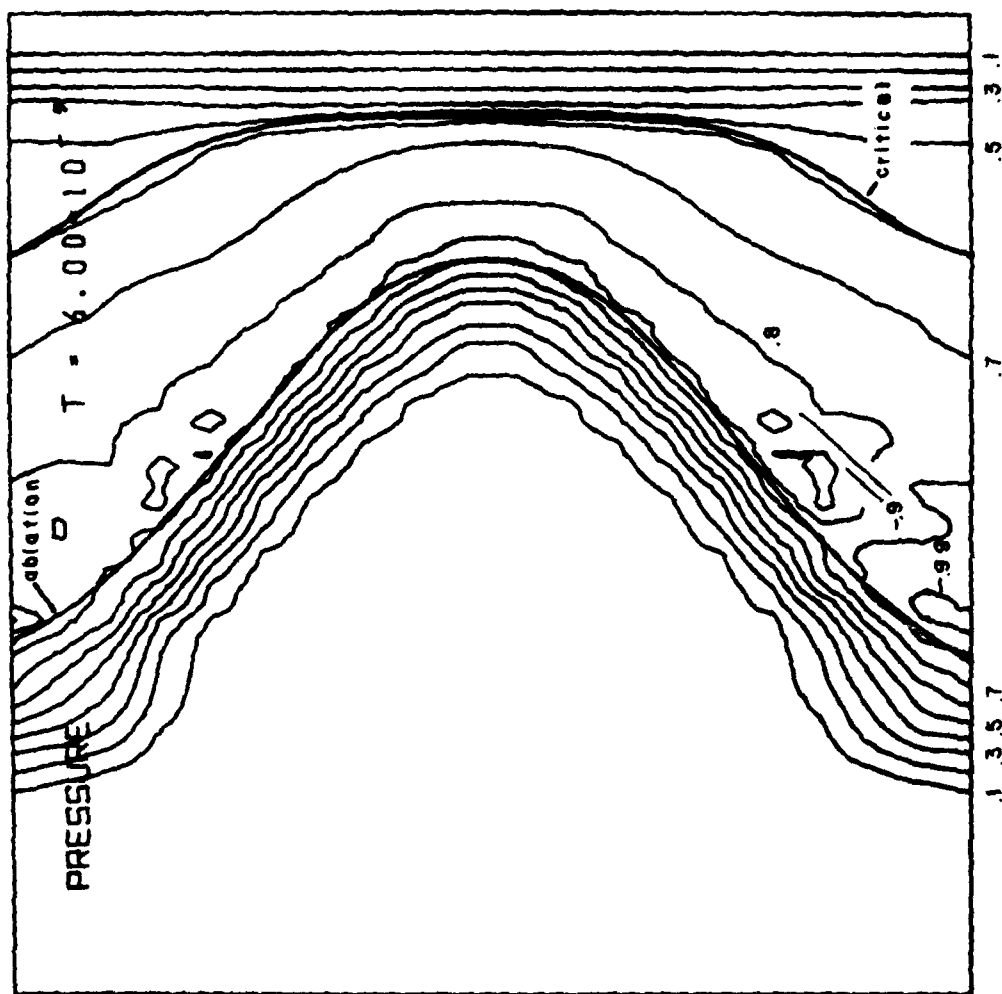
$\langle I \rangle = 1.0 \times 10^{13}$ W/cm^2

$\lambda_\ell = 600 \, \mu m$

Fig. 7 - Pressure contours for $\langle I \rangle = 1.0 \times 10^{13}$ W/cm^2 and $\lambda_\ell = 100 \, \mu m$ after 6 nanoseconds. The lines are contours of constant pressure in 0.10 increments of the maximum pressure. The critical and ablation surfaces are also indicated.

17

FAST2D LASER SHELL $6.00*10^{-9}$

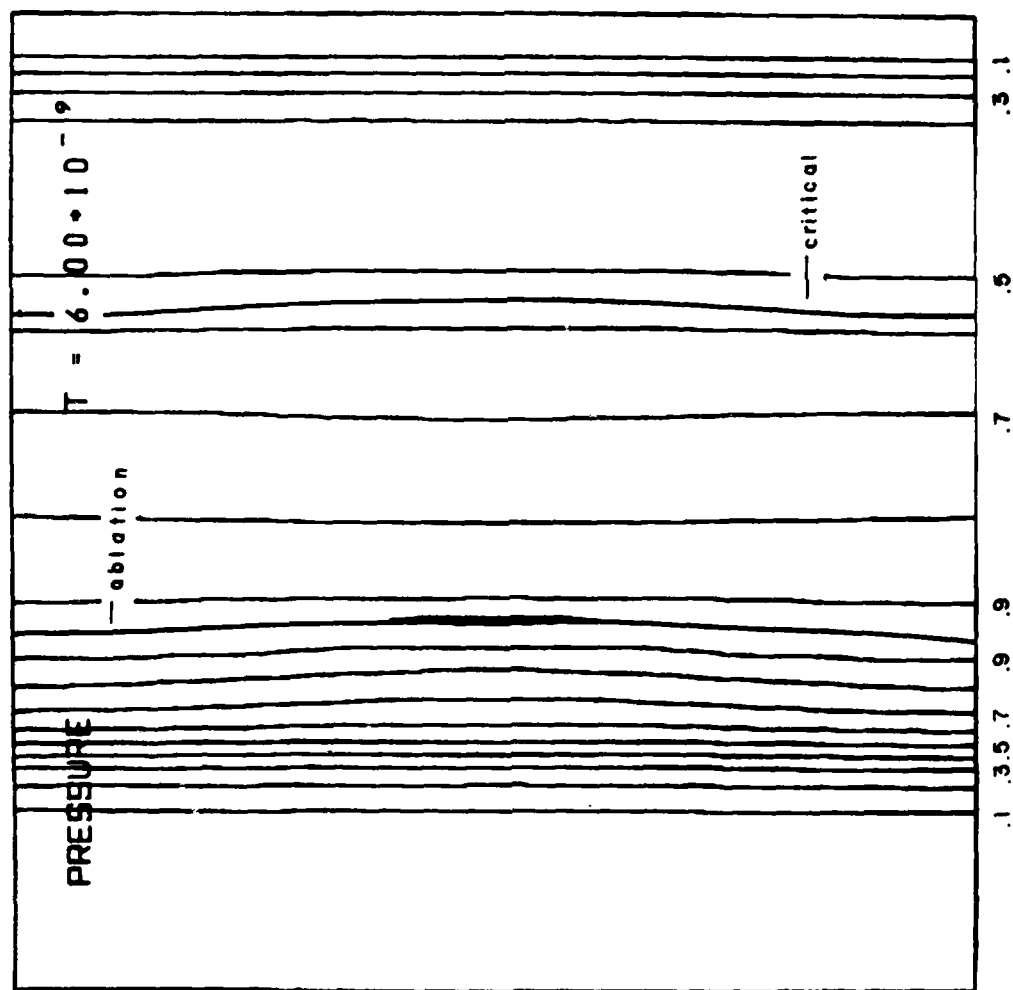$\langle I \rangle = 1.0 \times 10^{13}$ W/cm^2

$\lambda_\ell = 100\,\mu m$

Fig. 8 - The perspective density plot for $\langle I \rangle = 1.0 \times 10^{13}$ W/cm^2 and $\lambda_\ell = 100\,\mu m$ after 6 nanoseconds. At this short scalelength, very little distortion is observed.

18

Fig. 9 - Pressure contours for $\langle I \rangle = 1.0 \times 10^{13}$ W/cm^2 and $\lambda_\ell = 100$ μm after 6 nanoseconds
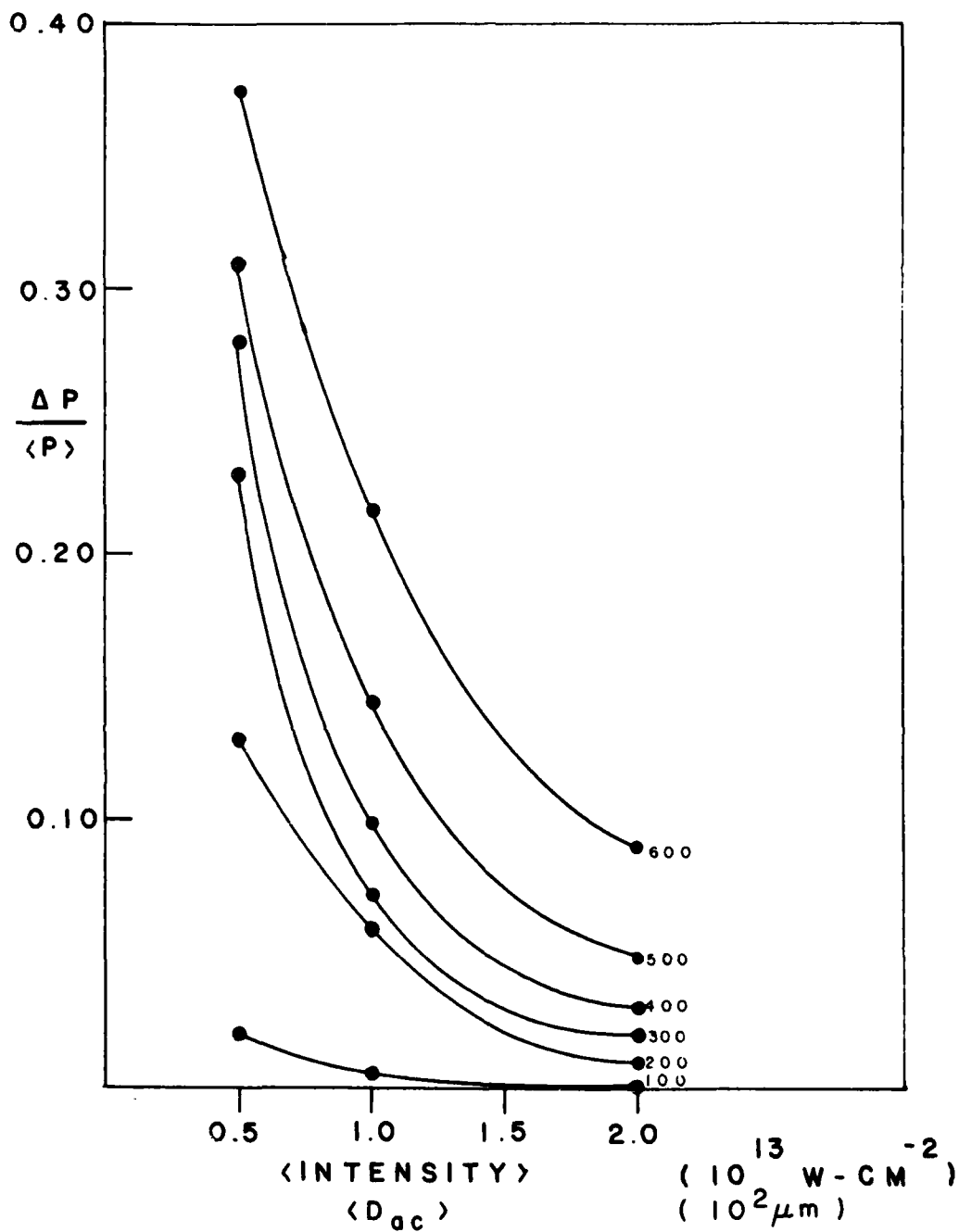
Fig. 10 - The variation in ablation pressure ($\Delta p / \langle p \rangle$) for all 6 scalelengths plotted as a function of the average laser intensity ($\langle I \rangle$) and as a function of the average distance from the ablation surface to the critical surface ($\langle D_{ac} \rangle$)